13E1-1 (Invited)

Fabrication and Applications of Deep Gratings Buried in Silica Glasses

Kenji Kintaka[1], Junji Nishii[1], Tatsuhiro Nakazawa[2], and Kazuaki Oya[2]
1: Photonics Research Institute, National Institute of Advanced Industrial Science and Technology (AIST),
1-8-31 Midorigaoka, Ikeda, Osaka 563-8577, Japan
Phone: +81-72-751-8527, Fax: +81-72-751-4027, E-mail: kintaka.kenji@aist.go.jp
2: Nippon Sheet Glass Co., Ltd.

Abstract: Our recent work is reviewed on fabrication of binary gratings with deep grooves and high spatial-frequency buried in silica glasses and on applications of such gratings to a wavelength demultiplexer and one-dimensional photonic crystals.

1. Introduction

Binary gratings with deep grooves and high spatial-frequency are very attractive elements in integrated optics because of their high diffraction efficiencies and birefringence properties. Polarization beam splitters, wave plates, and polarization-independent transmission diffraction devices can be realized by use of specially designed deep gratings. The microstructures of such deep gratings are, however, highly fragile and difficult to handle. Recently, we have demonstrated that deep gratings could be buried in silica plate by overcladding without decrease of diffraction efficiencies and polarization dependencies [1]. This paper reviews our recent work in fabrication and applications of the buried gratings.

2. Fabrication of buried gratings [1]

Surface-relief gratings were fabricated in a SiO_2 substrate by electron beam (EB) lithography and inductive coupled-plasma reactive ion etching (ICP-RIE). An 0.4-μm-thick EB resist (ZEP-520, Nippon Zeon) was spin-coated on a SiO_2 substrate, and grating pattern with 1.5-μm period was patterned by EB direct writing and developing. A 300-nm-thick Ni film was deposited by evaporation followed by liftoff. The Ni mask pattern was transferred to the SiO_2 substrate by ICP-RIE (RIE-200iP, Samco) with C_3F_8 gas. The residual Ni mask was removed by a $FeCl_3$ solution. Figure 1(a) shows a scanning electron microscope (SEM) photograph of the cross-sectional structure of the fabricated grating. The groove depth, the ratio of groove width to period, and the side slope were 2.8 μm, 0.4, and 88°, respectively. Small cracks near the top of grating teeth were due to cleaving of the sample for SEM observation.

The SiO_2 cladding layer was deposited on the surface-relief grating by plasma-enhanced chemical vapor deposition (PECVD) using $Si(OC_2H_5)_4$ as precursor. The substrate temperature, pressure, and rate in the deposition were 400 °C, 53 Pa, and 100 nm/min, respectively. Figure 1(b) shows a SEM photograph of the cross-sectional structure of the grating after the overcladding. Although the grating grooves had triangular shape at upper part, the groove widths of middle and lower parts were almost the same as those of the original grating.

Figure 2 shows 1st-order transmission diffraction efficiency of the gratings before and after the overcladding measured in the wavelength range from 1.5 to 1.58 μm with incident angle of 30°. Open and solid circles show diffraction efficiency of the original grating for TE and TM-polarized light, respectively.

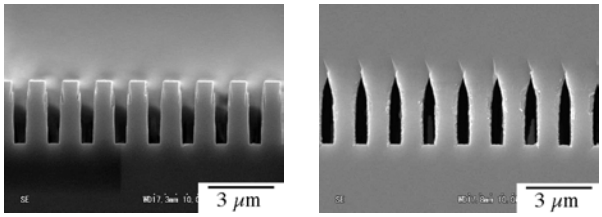

(a) (b)

Fig. 1. SEM photographs of deep gratings (a) before and (b) after overcladding.

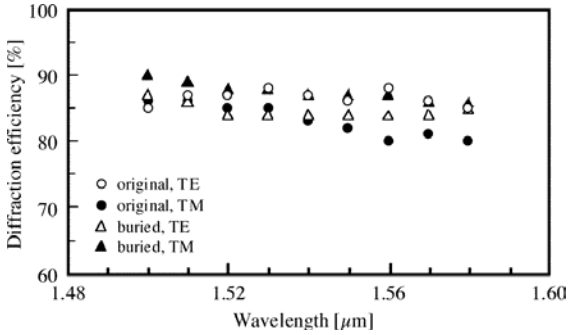

Fig. 2. Diffraction efficiency of the gratings before and after overcladding.

Open and solid triangles show diffraction efficiency of the buried grating for TE and TM-polarized light, respectively. Diffraction efficiencies higher than 80% were obtained with both gratings for TE and TM-polarized light, which were comparable with theoretically predicted values. Therefore, the deep grating can be successfully buried in SiO_2 by overcladding.

3. Coarse wavelength-division demultiplexer [2]

A compact four-channel demultiplexer using a high-spatial-frequency transmission grating buried in a silica-based waveguide have been proposed and investigated. A schematic view of the proposed demultiplexer with 20-nm wavelength spacing at 1550-nm band is illustrated in Fig. 3. The demultiplexer consists of a buried high-spatial-frequency transmission grating, a pair of parabolic mirrors, slab waveguide, and channel waveguides. The input light expands horizontally from the end of input channel waveguide to the slab waveguide, depending on the numerical aperture of the waveguide. The expanded light is reflected and collimated toward the buried grating by total internal reflection of the first parabolic mirror with an interface between the vertically etched waveguide and the air gap. The collimated light is diffracted by the buried grating. The 1st-order diffraction efficiency of the buried grating is more than 90 % across 200-nm bandwidth centred at 1550 nm. The diffracted light is reflected and focused onto the ends of the output channel waveguides by the

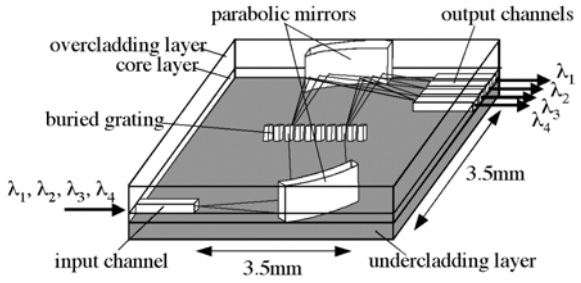

Fig. 3. Schematic view of the proposed 4-ch demultiplexer.

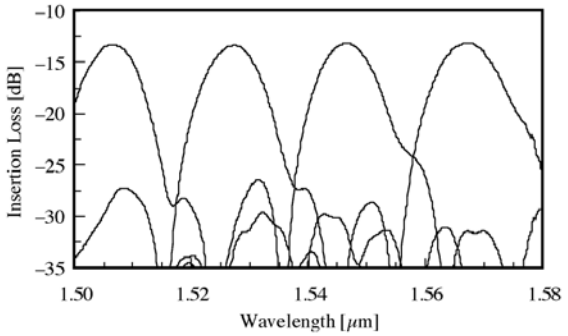

Fig. 4. Transmission spectrum of the 4-ch demultiplexer.

second parabolic mirror.

A 10-μm-thick SiO_2 undercladding and 5-μm-thick Ge-SiO_2 core layers were sequentially deposited on a SiO_2 substrate by PECVD. Channel waveguides of 5-μm width and a grating with 1.5-μm period, 5-μm groove depth, and 3.4-μm interaction length were patterned by EB lithography and ICP-RIE. A 10-μm-thick SiO_2 overcladding layer was deposited by PECVD. The parabolic mirrors were fabricated by photolithography and ICP-RIE. The device was annealed at 800 °C in air. The device size was 5.1 mm × 9.2 mm.

The device characteristics were measured by use of a wavelength-tunable laser diode, optical spectrum analyser, and single-mode fibers. The single-mode fibers were butt-coupled to input and output waveguides. Figure 4 shows transmission spectrum of the fabricated device. The average insertion loss was 13 dB, which includes coupling losses. The average crosstalk noise level was –16 dB for the adjacent channels. The polarization-dependent loss (PDL) was about 0.6 dB. The insertion loss and PDL will be reduced by optimization of the fabrication condition.

4. Triangular one-dimensional photonic crystals [3, 4]

Novel wavelength-division devices using triangular one-dimensional photonic crystals (1D-PhCs) buried in glass substrates have been proposed and investigated for realization of large angular dispersion. Figure 5 illustrates a schematic view of the proposed device consisting of Ta_2O_5 core and SiO_2 cladding [4]. The input and output surfaces were tilted at an angle of 45° from the grating vector, so that the incident beam could be coupled with the first photonic band in the second Brillouin zone. The grating period and incident angle were designed to be 500 nm and 10°, respectively.

A 3-μm-thick Ta_2O_5 core layer was deposited on a SiO_2 substrate by RF ion plating (NSG Techno-Research). The grating with 3-μm-deep grooves was fabricated by two-beam interference exposure and ICP-RIE with CHF_3 gas. A 10-μm-

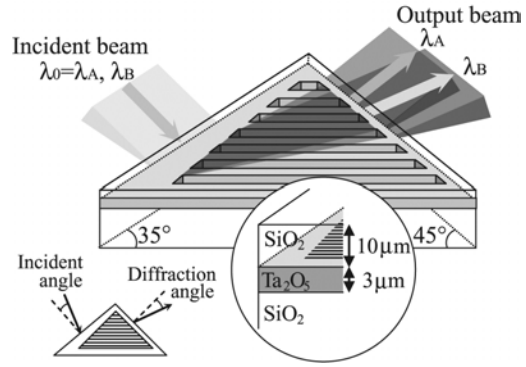

Fig. 5. Schematic view of the triangular 1D-PhC.

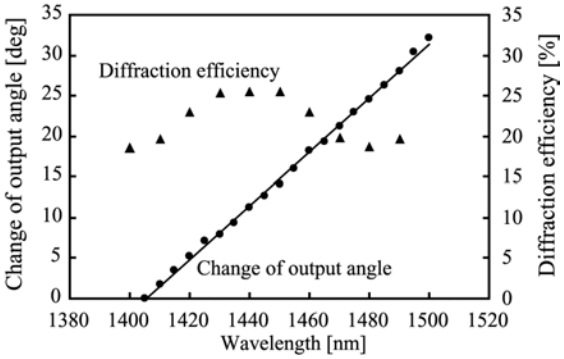

Fig. 6. Wavelength dependencies of diffraction efficiency (solid triangles) and change of output angle (solid circles).

thick SiO_2 over-cladding layer was deposited by PECVD.

TM mode was end-coupled in the slab waveguide through a selfoc microlens and a rod lens. Figure 6 shows the wavelength dependencies of diffraction efficiency and the change of output angle, which indicates the angular difference from that at 1405 nm in wavelength. The output angle change was 4.8° with the incident wavelength change of 1% in wavelength range from 1400 to 1500 nm, which was six times as large as that of conventional gratings. A maximum diffraction efficiency of 25% was obtained at around 1440-nm wavelength. Higher diffraction efficiency will be obtained by improving of the fabrication accuracy.

5. Conclusions

We have fabricated deep gratings with high spatial-frequency buried in silica-based glasses, and applied these gratings to the wavelength demultiplexer and the triangular 1D-PhCs.

Acknowledgement

This work was conducted in the Nanotechnology Glass Project as part of the Nanotechnology Materials Program supported by the New Energy and Industrial Technology Development Organization (NEDO).

References

1 J. Nishii *et al*., Appl. Opt., **43**, pp.1327-1330 (2004).
2 T. Nakazawa *et al*., Opt. Lett., **29**, pp.1188-1190 (2004).
3 K. Oya *et al*., Opt. Lett., **30**, pp.192-194 (2005).
4 K. Oya *et al*., Jpn. J. Appl. Phys., **45**, pp.L1001-L1003 (2006).